

## **Thermal-Mechanical Buckling Analysis of Laminated Composite Shells by Finite Element Method**

J. Li<sup>1</sup>, Z.H. Xiang<sup>1</sup> and M.D. Xue<sup>1</sup>

### **Summary**

This paper presents a finite element scheme to analyze the buckling behavior of composite shells subjected to thermal and mechanical loads. Firstly, a kind of multi-layered composite shell element with relative degrees-of-freedom is adopted to model laminated composite shells. Then the corresponding temperature element is developed so that the mechanical analysis and the thermal analysis share a common mesh. Moreover, a new criterion of critical heat flux is proposed in stead of the traditional criterion of critical temperature. Finally, the advantage of the proposed scheme is illustrated by calculating the stable region of thermal-mechanical loads for a honeycomb sandwich composite cylinder.

### **Introduction**

Laminated composites are widely used in modern engineering structures due to their good specific properties. Sometimes these composites may work in severe conditions, where not only mechanical but also thermal loads are applied. Consequently, the buckling behavior of these structures under thermal-mechanical loading has drawn many researchers' attention. In this paper, a Finite Element (FE) scheme is presented for this purpose.

The buckling analysis of composite structures has been extensively studied over years [1, 2]. Many methods are based on layer wise theories [3] or two dimensional shell theories. Although these methods can give good solutions to the global buckling behavior, they still have some shortcomings, such as: difficult to be connected with solid elements which are necessary to modeling joints, fringes, etc.; too rigid if using low order shell theories and too complex if using high order shell theories; difficult to calculate the transverse shear stress accurately if using the layer wise theories. To overcome these shortcomings, a kind of shell element with Relative Degrees-of-Freedom (RDOF) and Wilson's incompatible inner Degrees-of-Freedom (DOF) was proposed in Ref. [4]. Because it is actually a kind of solid element, it is easy to be connected with other solid elements. With this element, the local buckling behavior of honeycomb sandwich shells reinforced by aluminum frames was successfully simulated in Ref. [4]. Then this element was improved in Ref. [5] to model multi-layered composites with arbitrary number of laminae and was used to study the influence of cutouts on the buckling behavior of composite shells [6]. Owing to the good performance of this element, it is adopted in this paper.

---

<sup>1</sup>Department of Engineering Mechanics, Tsinghua University, Beijing, 100084, P. R. China

In the FE formulation, temperature strains are the direct products of the thermal expansion coefficient and the temperature difference. Because the mechanical strains are functions of the derivatives of displacements, the order of the displacement shape function should be one times higher than that of the temperature shape function, so that these two kinds of strains are compatible with each other. In the present FE scheme, the displacement multi-layered shell elements contain the Wilson incompatible inner DOFs, which are not existed in the corresponding temperature shell elements. This automatically satisfies the aforementioned compatibility requirement.

In the traditional concept of thermal buckling, the temperature is assumed being uniformly distributed over the whole structure, and the buckling occurs when the temperature reaches a critical value. However, the uniform distribution of temperature is a strong assumption, which is hard to be satisfied in practice. Therefore, the critical heat flux is proposed instead of the traditional critical temperature in this paper.

### The Multi-Layered Composite Shell Element

Fig. 1 shows an  $n$ -layered shell element, which is a combination of  $n$  layers of 16-noded incompatible element with RDOF [4]. The transformations of nodal coordinates and nodal displacements of the  $k$ th layer are defined as:

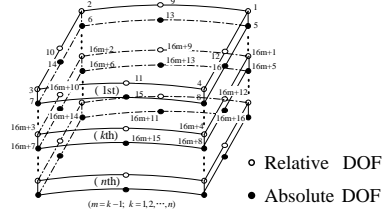


**Figure 1:** Multi-layered shell element with RDOF

$$\begin{cases} {}^k\bar{\mathbf{x}}_i = {}^k\mathbf{x}_i - {}^k\mathbf{x}_{i+4} \\ {}^k\bar{\mathbf{x}}_{i+4} = {}^k\mathbf{x}_{i+4} \end{cases} \quad \begin{cases} {}^k\bar{\mathbf{u}}_i = {}^k\mathbf{u}_i - {}^k\mathbf{u}_{i+4} \\ {}^k\bar{\mathbf{u}}_{i+4} = {}^k\mathbf{u}_{i+4} \end{cases} \quad \begin{matrix} i = 16(k-1) + j \\ j = 1, 2, 3, 4, 9, 10, 11, 12 \end{matrix} \quad (1)$$

where  $i$  is the node number;  $\mathbf{x}_i$  is the nodal coordinate vector;  $\mathbf{u}_i$  is the nodal displacement vector;  $\bar{\mathbf{x}}_i$  is the nodal relative coordinate vector and  $\bar{\mathbf{u}}_i$  is the nodal relative displacement vector. The corresponding shape function  $\bar{N}_i$  is:

$$\bar{N}_i = N_i \quad \bar{N}_{i+4} = N_i + N_{i+4} \quad i = 1, 2, 3, 4, 9, 10, 11, 12 \quad (2)$$

where  $N_i$  is the shape function of ordinary 16-noded brick element [7]. This 16-noded element is further improved by adding the Wilson's inner additional DOFs. Details can be found in Refs. [4-6].

Connecting these 16-noded elements layer by layer obtains the continuous conditions shown in Eq. (3). These conditions can be incorporated into the total potential energy of the system by the Lagrange multiplier method. In this way, the

redundant DOFs between each layer can be eliminated [5, 6].

$$\begin{aligned} {}^{k-1}\bar{\mathbf{u}}_i &= {}^k\bar{\mathbf{u}}_j + {}^k\bar{\mathbf{u}}_{j+4} \\ i &= m+5, m+6, m+7, m+8, m+13, m+14, m+15, m+16 \\ k &= 2, \dots, n \quad m = 16(k-2) \quad j = i+12 \end{aligned} \quad (3)$$

Based on the same idea, the corresponding temperature element can be constructed by replacing  $\mathbf{u}_i$  and  $\bar{\mathbf{u}}_i$  with the absolute and relative nodal temperature  $\varphi_i$  and  $\bar{\varphi}_i$ , respectively, in the above equations. However, the Wilson's additional inner DOFs are not used, so that the order of temperature strains and mechanical strains are compatible with each other.

The above mechanical and temperature elements can be used to analyze composite shells, if the anisotropic material properties are considered. Because these two kinds of elements share the same mesh, there is no extrapolation errors introduced during the thermal-structural analysis.

### **The Formulation of Thermal-Mechanical Buckling Analysis**

In this paper, the FE formulation of linear-elastic buckling is based on the following assumptions:

1. Thermal and mechanical loads are independent of the structural deformation;
2. The steady incremental temperature  $\varphi$  is proportional to the heat flux  $\mathbf{q}$ , i.e.  $\mathbf{K}_T \varphi = \mathbf{q}$ , where  $\mathbf{K}_T$  is the heat conduction matrix;
3. All material properties are independent of the temperature and time;
4. The structure is linear before buckling.

From assumption (b), the load  $\mathbf{Q}_T$ , which is due to thermal expansion  $\varepsilon_T$ , is proportional to the heat flux:

$$\mathbf{Q}_T = \int_v \mathbf{B}_{L0}^T \mathbf{D} \varepsilon_T dV = \int_v \mathbf{B}_{L0}^T \mathbf{D} \alpha dV \varphi = \left( \int_v \mathbf{B}_{L0}^T \mathbf{D} \alpha dV \mathbf{K}_T^{-1} \right) \mathbf{q} \quad (4)$$

where  $\mathbf{B}_{L0}$  is the strain matrix;  $\mathbf{D}$  is the elasticity matrix and  $\alpha$  is the thermal expansion coefficient matrix.

With above assumptions, the Total Lagrange formulation of the large displacement FE equation at iteration time  $t + \Delta t$  is expressed as [7]:

$$({}^t\mathbf{K}_{L0} + {}^t\mathbf{K}_u + {}^t\mathbf{K}_\sigma) \Delta \mathbf{a} = {}^{t+\Delta t}\mathbf{Q} - {}^t\mathbf{F} \quad (5)$$

where  $\Delta \mathbf{a}$  is the incremental displacement vector;  ${}^t\mathbf{K}_{L0}$  is the linear-elastic stiffness matrix;  ${}^t\mathbf{K}_u$  is the linear initial-displacement stiffness matrix;  ${}^t\mathbf{K}_\sigma$  is the initial-stress stiffness matrix;  ${}^{t+\Delta t}\mathbf{Q}$  is the load vector at time  $t + \Delta t$ ;  ${}^t\mathbf{F}$  is the load vector corresponding to the stresses at time  $t$ .

Suppose external loads could be divided into a constant load  $\mathbf{Q}_c$  and a variable load  $\mathbf{Q}_v$ .  $\mathbf{Q}_v$  is in pattern  $\mathbf{Q}_v^0$  and the critical load  $\mathbf{Q}_v^c = \lambda \mathbf{Q}_v^0$  ( $\lambda > 1$ ). Here  $\mathbf{Q}_c$  and  $\mathbf{Q}_v$  could be thermal or mechanical loads or their combinations. From assumption (d), the following relations read at time  $t$ :

$${}^t\mathbf{K}_{L0}\mathbf{u}_c = \mathbf{Q}_c \quad {}^t\mathbf{K}_{L0}\lambda\mathbf{u}_v^0 = \lambda\mathbf{Q}_v^0 \quad (6)$$

At time  $t + \Delta t$ ,  $\mathbf{Q}_v$  increases to  $(\lambda + \Delta\lambda)\mathbf{Q}_v^0$ , and Eq. (5) can be rewritten as:

$$[{}^t\mathbf{K}_{L0} + {}^t\mathbf{K}_u(\mathbf{u}_c + \lambda\mathbf{u}_v^0) + {}^t\mathbf{K}_\sigma(\sigma_c + \lambda\sigma_v^0)]\Delta\mathbf{a} = \mathbf{Q}_c + (\lambda + \Delta\lambda)\mathbf{Q}_v^0 - {}^t\mathbf{F}_c - \lambda{}^t\mathbf{F}_v^0 \quad (7)$$

where  $\sigma_c$  and  $\sigma_v^0$  correspond to  $\mathbf{Q}_c$  and  $\mathbf{Q}_v^0$ , respectively. Because  ${}^t\mathbf{F}_c = \mathbf{Q}_c$ ,  ${}^t\mathbf{F}_v^0 = \mathbf{Q}_v^0$  and  $\Delta\lambda = 0$  at the critical point, the following buckling equation can be obtained from Eq. (7):

$$\{ {}^t\mathbf{K}_{L0} + {}^t\mathbf{K}_u(\mathbf{u}_c) + {}^t\mathbf{K}_\sigma(\sigma_c) + \lambda [{}^t\mathbf{K}_u(\mathbf{u}_v^0) + {}^t\mathbf{K}_\sigma(\sigma_v^0)] \} \Delta\mathbf{a} = 0 \quad (8)$$

### Examples

The validity of the proposed method has been checked by a simple example in Ref. [8]. However, it is omitted here due to the page limits. The advantage of this method is illustrated by the example shown Fig. 2. The thickness of the aluminum honeycomb core is 10 mm, which is covered by outer and inner Kevlar fiber reinforced panels of 0.5 mm in thickness. The outer surface is subjected to lateral heat flux  $q$  and mechanical pressure  $p$ . The inner surface is the convection boundary with the convection coefficient of  $8.0 \text{ W/m}^2\cdot\text{K}$ . The environment temperature is  $0^\circ\text{C}$ . The temperature at the bottom of the cylinder is fixed to  $0^\circ\text{C}$ . The top of the cylinder is adiabatic. Both bottom and top are fixed. This cylinder is modeled by three-layered shell element presented in the previous text. There are 36 elements in the axial direction and 200 elements along the circumference. During the analysis, the material properties were taken from Table 1.

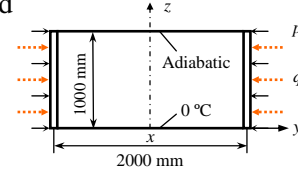


**Figure 2:** Honeycomb sandwich composite cylinder

Fig. 3 shows the first buckling modes of the pure mechanical loading and the pure thermal loading cases, where the critical pressure and heat flux are  $p_c = 4.778 \times 10^{-2} \text{ MPa}$  and  $q_c = 1681 \text{ W/m}^2$ , respectively. It is observed that the critical temperature reaches  $235^\circ\text{C}$ , under which the resin may melt. This indicates that the actual critical heat flux should be lower than the calculated one.

Fig. 4 shows the stable region of combined loading cases. These data were obtained by letting the thermal load be variable while fixing the pressure  $p$  at different levels. It observes that larger the pressure, smaller the critical heat flux. That means

Table 1: The material properties of the honeycomb sandwich composite cylinder

Mechanical	$E_1 = E_2$ (GPa)	$E_3$ (GPa)	$G_{12}$ (GPa)	$G_{23} = G_{13}$ (GPa)	$\nu_{12}$	$\nu_{23}$	$\nu_{13}$
Surface	15.0	1.72	5.37	1.57	0.28	0.034	0.3
Core	$2.5 \times 10^{-4}$	0.12	$0.9 \times 10^{-4}$	0.13	0.35	0.3	$6.25 \times 10^{-4}$
Thermal	$\alpha_1$ ( $10^{-6}/^\circ\text{C}$ )	$\alpha_2 = \alpha_3$ ( $10^{-6}/^\circ\text{C}$ )	$k_x$ (W/m·K)	$k_y$ (W/m·K)	$k_z$ (W/m·K)		
Surface	10.3	79.0	11.56	11.56	0.78		
Core	24.9	24.9	1.13	1.13	1.51		

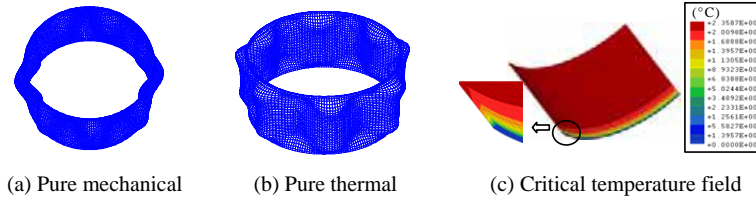


Figure 3: First buckling modes of unitary loading cases

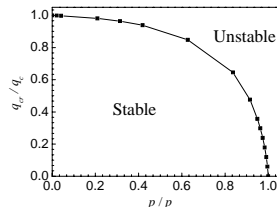
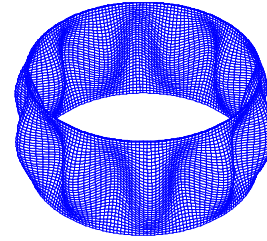


Figure 4: Stable region of combined load-cases



( $p/p_c = 0.36; q_c/q_c = 0.95$ )

Figure 5: A typical buckling mode

if lateral pressure is added, thermal buckling will happen before the melting point. The influence of the lateral pressure is also presented by comparing the buckling modes in Fig. 3(b) and Fig. 5. It seems that adding lateral pressure will change the distribution of wave numbers in the buckling mode.

### Conclusion

With the proposed FE scheme in this paper, it is possible to study the influence of the combination of thermal and mechanical loads on the structural buckling behaviors. Because RDOF shell elements and a common mesh are used for the thermal and mechanical analyses, it is easy to model complex structures in practice with high accuracy. However, further work should be carried out to consider the temperature dependent material properties.

### References

1. Noor, A. K. and Burton W. S. (1990): "Assessment of Computational Models for Multilayered Composite Shells", *Applied Mechanics Reviews*, Vol. 43,

pp. 67-97.

2. Idlbi, A., Karama, M. and Touratier, M. (1997): "Comparison of Various Laminated Plate Theories", *Computers and Structures*, Vol. 37, pp. 173-184.
3. Reddy, J. N. (1993): "An Evaluation of Equivalent Single Layer and Layer-wise Theories of Composite Laminates", *Computers and Structures*, Vol. 25, pp. 21-58.
4. Xiang, Z. H., Xue M. D. and Cen Z. Z. (2002): "Finite Element Buckling Analysis of Rotationally Periodic Laminated Composite Shells", *International Journal for Numerical Methods in Engineering*, Vol. 53, pp. 959-981.
5. Li, J., Xiang, Z. H. and Xue, M. D. (2005): "Buckling Analysis of Rotationally Periodic Laminated Composite Shells by a new Multilayered Shell Element", *Composites Structures*, Vol. 70, pp. 24-32.
6. Li, J., Xiang, Z. H. and Xue, M. D. (2005): "Three-Dimensional Finite Element Buckling Analysis of Honeycomb Sandwich Composite Shells with Cutouts", *Computers, Materials & Continua*, Vol. 2, pp. 139-150.
7. Bath, K. J. (1996): *Finite Element Procedures*, Prentice Hall.
8. Huang, N. N., Taucher, T. R. (1990): "Thermal Buckling of Clamped Symmetric Laminated Plates", *ASME, Aerospace Division*, Vol. 20, pp. 53-59.